Study of the $\pi^0\pi^0\eta'$ final state in $\bar{p}p$ annihilation at rest

Crystal Barrel Collaboration

A. Abele [h], J. Adomeit [g], C. Amsler [p], C.A. Baker [e], B.M. Barnett [c], C.J. Batty [e], M. Benayoun [m], A. Berdoz [n], K. Beuchert [b], S. Bischoff [h], P. Blüm [h], K. Braune [l], J. Brose [k], D.V. Bugg [i], T. Case [a], A. Cooper [i], O. Cramer [l], V. Credé [c], K.M. Crowe [a], T. Degener [b], N. Djaoshvili [l], S. v. Dombrowski [p], M. Doser [f], W. Dünnweber [l], A. Ehmanns [c], D. Engelhardt [h], M.A. Faessler [l], P. Giarritta [p], R. Hackmann [c], R.P. Haddock [j], F.H. Heinsius [a], M. Heinzelmann [p], M. Herz [c], N.P. Hessey [l], P. Hidas [d], C. Hodd [i], C. Holtzhaußen [h], D. Jamnik [l,1], H. Kalinowsky [c], B. Kämmle [g], P. Kammel [a], T. Kiel [h], J. Kisiel [f,2], E. Klempt [c], H. Koch [b], C. Kolo [l], M. Kunze [b], M. Lakata [a], R. Landua [f], J. Lüdemann [b], H. Matthäy [b], R. McCrady [n], J. Meier [g], C.A. Meyer [n], L. Montanet [f], A. Noble [p,3], R. Ouared [f], F. Ould-Saada [p], K. Peters [b], B. Pick [c], C. Pietra [p], C.N. Pinder [e], G. Pinter [d], C. Regenfus [l], S. Resag [c,4], W. Roethel [l], P. Schmidt [g], I. Scott [i], R. Seibert [g], S. Spanier [p,5], H. Stöck [b], C. Straßburger [c], U. Strohbusch [g], M. Suffert [o], U. Thoma [c], M. Tischhäuser [h], D. Urner [p], C. Völcker [l], F. Walter [k], D. Walther [b], U. Wiedner [f], B.S. Zou [i]

[a] *University of California, LBNL, Berkeley, CA 94720, USA*

[b] *Universität Bochum, D-44780 Bochum, FRG*

[c] *Universität Bonn, D-53115 Bonn, FRG*

[d] *Academy of Science, H-1525 Budapest, Hungary*

[e] *Rutherford Appleton Laboratory, Chilton, Didcot OX11 0QX, UK*

[f] *CERN, CH-1211 Geneva 4, Switzerland*

[g] *Universität Hamburg, D-22761 Hamburg, FRG*

[h] *Universität Karlsruhe, D-76021 Karlsruhe, FRG*

[i] *Queen Mary and Westfield College, London E1 4NS, UK*

[j] *University of California, Los Angeles, CA 90024, USA*

[k] *Universität Mainz, D-55099 Mainz, FRG*

[l] *Universität München, D-80333 München, FRG*
[m] *LPNHE Paris VI, VII, F-75252 Paris, France*
[n] *Carnegie Mellon University, Pittsburgh, PA 15213, USA*
[o] *Centre de Recherches Nucléaires, F-67037 Strasbourg, France*
[p] *Universität Zürich, CH-8057 Zürich, Switzerland*

A partial wave analysis of $\bar{\mathrm{p}}\mathrm{p}\to\pi^0\pi^0\eta'$ has been performed using the $\eta'\to\pi^0\pi^0\eta$ and $\eta'\to\gamma\gamma$ decay modes. The data are dominated by an η' recoiling against the $(\pi\pi)$ S-wave. In addition, $a_2(1320)\to\eta'\pi^0$ is needed. There is evidence for contributions from $a_0(1450)\to\eta'\pi^0$. The branching ratio of $a_0(1450)\to\eta'\pi^0$ with respect to $\eta\pi^0$ is consistent with the prediction of SU(3).

We have reported the observation of a new scalar resonance, the $a_0(1450)$ [1]. This state was required to describe the process $\bar{\mathrm{p}}\mathrm{p}\to\pi^0\pi^0\eta\to6\gamma$ at rest in liquid hydrogen. The most prominent structures in the $\pi^0\pi^0\eta$ final state were $a_0(980)$ and $a_2(1320)$. In addition, there were significant contributions from the $(\pi\pi)$ S-wave, which contains the $f_0(980)$ and another scalar meson at (1300 - 1400) MeV, the $f_0(1370)$. Coupled channel analyses also need the $a_0(1450)$ meson [2,3]. In this letter, we present an analysis of the related reaction $\bar{\mathrm{p}}\mathrm{p}\to\pi^0\pi^0\eta'$, $\eta'\to\pi^0\pi^0\eta$ and $\eta'\to\gamma\gamma$. This final state allows the same resonances as $\pi^0\pi^0\eta$, but the phase space is more restricted. The branching ratios of resonances in the $\pi^0\pi^0\eta'$ channel will be compared to $\pi^0\pi^0\eta$ and the predictions from SU(3)-flavour. In this context the $a_2(1320)$ and the $a_0(1450)$ are of special interest.

The main selection criteria and cuts follow closely those used previously to select the $5\pi^0\to10\gamma$ [4] and the $\pi^0\eta\eta'\to6\gamma$ final state [5]. The data were obtained by stopping antiprotons from LEAR in the liquid hydrogen target of the Crystal Barrel detector. A detailed description of the detector is given in [6]. A total of about $16.8\cdot10^6$ annihilations were recorded using an all-neutral trigger which required no charged tracks in the two PWC's surrounding the target. After removing residual events containing charged tracks (due to trigger inefficiencies, for example from $K_s\to\pi^+\pi^-$) events with 10 or 6 electromagnetic showers with a minimum energy deposit of 20 MeV in the barrel were selected.

[1] University of Ljubljana, Ljubljana, Slovenia
[2] University of Silesia, Katowice, Poland
[3] Now at CRPP, Ottawa, Canada
[4] Part of this work appears in the Ph.D. thesis of S. Resag
[5] Email contact: stefan.spanier@cern.ch

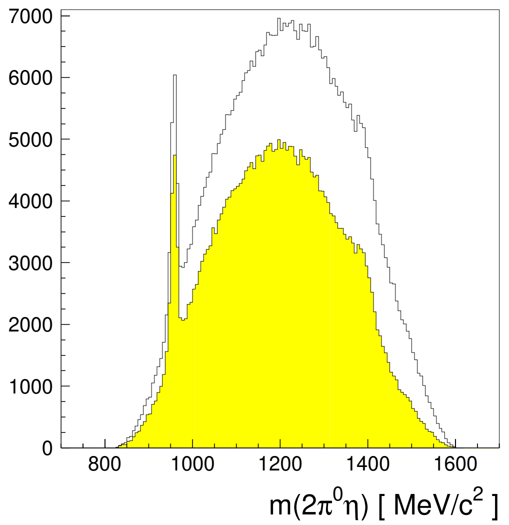

Fig. 1.
The $2\pi^0\eta$ mass distribution before (white) and after (grey) removing $\bar{p}p\to\pi^0\eta\eta$ events.

To avoid energy leakage showers were not allowed to appear at the edges of the calorimeter. The data sample was further reduced by the constraint that the total energy deposit of all photons had to lie close to $2m_pc^2$. Hence, we collected $1.08\cdot10^6$ ten-photon and $1.65\cdot10^6$ six-photon events. Both samples were then subjected to a kinematic fit requiring energy and momentum conservation with a probability greater than 1%, leaving $7.7\cdot10^5$ ten-photon and $1.5\cdot10^6$ six-photon events.

We proceed with the description of the selection for the 10γ data, which provide the higher statistics sample for the $\pi^0\pi^0\eta'$ final state: The 10γ events were kinematically fitted to the hypotheses $\bar{\mathrm{p}}\mathrm{p}\to5\pi^0$ and $\bar{\mathrm{p}}\mathrm{p}\to4\pi^0\eta$. Ambiguous events (20%) were assigned to these hypotheses according to their respective confidence level, which were weighted with the corresponding branching ratios. In the invariant 2γ-mass spectrum there is no evidence for any background from $\eta'\to2\gamma$ or from $\omega\to\pi^0\gamma$ with a soft missing photon.

The invariant $2\pi^0\eta$ mass distribution of the $4\pi^0\eta$ final state (fig. 1) exhibits two interesting structures. A clear η' signal is visible due to events of the type $\bar{\mathrm{p}}\mathrm{p}\to2\pi^0\eta'$, $\eta'\to\pi^0\pi^0\eta$. The signal sits on a non-negligible background. This background is reduced by removing $\pi^0\eta\eta$ ($\eta\to3\pi^0,\eta\to\gamma\gamma$) events (grey histogram of fig. 1). The second structure appears at a $\pi^0\pi^0\eta$ mass of about 1400 MeV. A similar structure has been observed in our $\pi^+\pi^-\pi^0\pi^0\eta$ data, in both $\pi^0\pi^0\eta$ and $\pi^+\pi^-\eta$ mass distributions; it was found to be generated by the $\eta(1440)$ (E/ι) meson [7].

Here we analyse the clear $\eta'(\to\pi^0\pi^0\eta)$ signal (8230 events) due to $\bar{\mathrm{p}}\mathrm{p}\to\pi^0\pi^0\eta'$ events. The description of the background under the signal (5970 events) is based on the assumption that it produces the same distribution in the Dalitz plot as events lying in 'side-bins'. For the η' signal we use a mass window from 945 MeV to 969 MeV. By 'side-bins' we mean the regions in the invariant $\pi^0\pi^0\eta$ mass distribution below the peak (from 927 MeV to 939 MeV) and above (975 MeV to 987 MeV). Thus we expect to have the same number of events in the two side-bins and under the η' signal. To shift the side-bin events into the kinematic borders of the $\pi^0\pi^0\eta'$ Dalitz plot, the background events are kinematically fitted to the hypothesis $\pi^0\pi^0\eta'$. Before kinematic fitting, energy and momentum are multiplied by a scaling factor so that the invariant $\pi^0\pi^0\eta$ mass is exactly the η' mass.

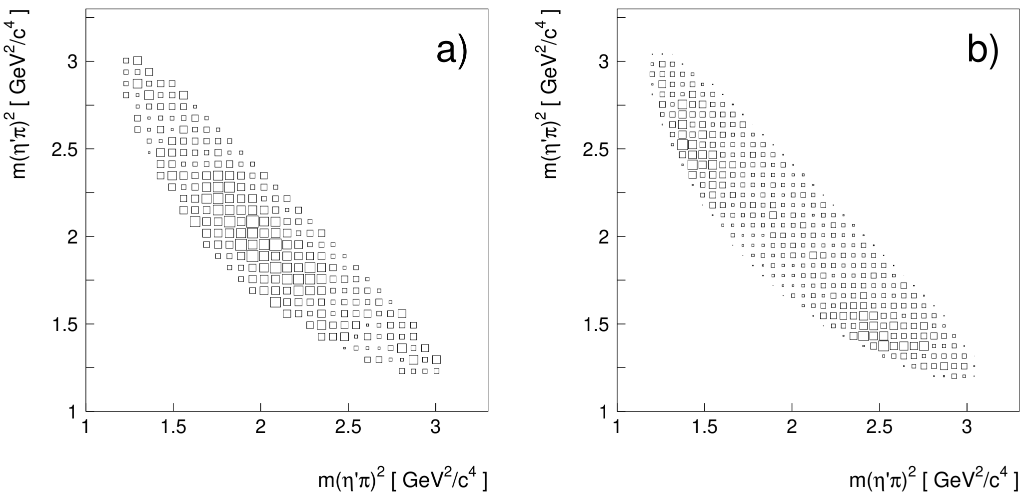

Fig. 2. *The $\pi^0\pi^0\eta'$ ($\eta'\to\pi^0\pi^0\eta$) Dalitz plot, a) in the signal region, background and acceptance corrected, and b) generated from 'side-bin' events.*

The final Dalitz plot (fig. 2a)) is generated by subtracting the side-bin Dalitz plots (fig. 2b)) from the signal Dalitz plot. The background Dalitz plot of fig. 2b shows a structure which also appears in the data plot of fig. 2a at $m^2(\eta'\pi^0_1) = 2.4 \cdot 10^6$ MeV^2 and $m^2(\eta'\pi^0_2) = 1.4 \cdot 10^6$ MeV^2. The $\pi^0\pi^0\eta'$ Monte Carlo data demonstrate that these events come from wrong $\pi^0\pi^0\eta$ combinations which happen to have a mass close to the η'. In all other parts of the Dalitz plot the background is nearly flat. Only 18% of the background can be assigned to combinatorial background while the main part is due to $4\pi^0\eta$ events not forming an η'. Phase-space-distributed $4\pi^0\eta$ events do not cause any significant structures in the $\pi^0\pi^0\eta'$ Dalitz plot. The detector acceptance is estimated from $\pi^0\pi^0\eta'$ Monte Carlo events; these are treated in exactly the same way as real data. The branching ratio is evaluated from the strength of the $\pi^0\pi^0\eta'$ signal, the number of $\bar{p}$ stopping in the LH_2 target and a Monte Carlo determination of the detection efficiency (9.1±0.1 %). The number of all-neutral events is scaled to those observed with an open trigger requiring $\bar{p}$ stops only (enrichment factor 25).

The procedure to select the 6-photon data is next described: The $1.65 \cdot 10^6$ events after preselection were fitted kinematically to the following hypotheses which consist of combinations of the mesons $\pi^0(\to\gamma\gamma)$, $\eta(\to\gamma\gamma)$, $\eta'(\to\gamma\gamma)$ and $\omega(\to\pi^0\gamma\to3\gamma)$ leading finally to the 6 photons: (7C) $\pi^0\pi^0\pi^0$, $\pi^0\pi^0\eta$, $\pi^0\eta\eta$, $\pi^0\pi^0\eta'$, $\pi^0\pi^0\eta'$, $\pi^0\eta\eta'$; (8C) $\omega\omega$; (6C) $\pi^0\pi^0\gamma\gamma$ and $\pi^0\eta\gamma\gamma$. The strongest chan-

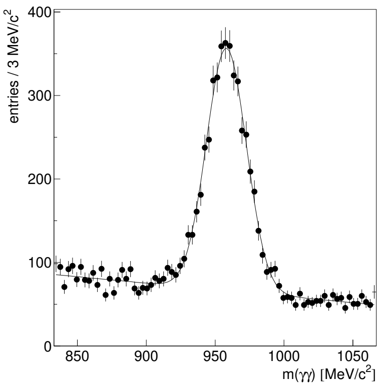

Fig. 3.
The $\gamma\gamma$ invariant mass distribution in the η' region after the 6C kinematic fit to $\pi^0\pi^0\gamma\gamma$.

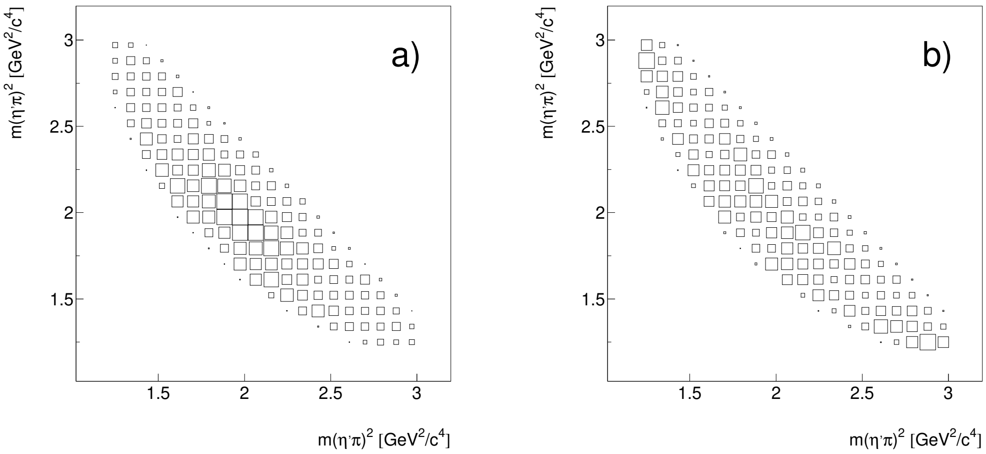

Fig. 4. *The $\pi^0\pi^0\eta'\,(\eta'\to\gamma\gamma)$ Dalitz plot, a) after background subtraction and acceptance correction and b) generated from 'side-bin' events.*

nels ($3\pi^0$, $\pi^0\pi^0\eta$ and $\pi^0\eta\eta$) were suppressed by rejecting events where these channels had the highest confidence level. In addition the 6C-fit to $\pi^0\pi^0\gamma\gamma$ had to have at least 10% probability while not exceeding 1% for the hypothesis $\pi^0\eta\gamma\gamma$. The $\gamma\gamma$ invariant mass of the residual photon pair is shown in fig. 3.

In the mass window 900 MeV/c^2 $< m(\gamma\gamma) <$ 1020 MeV/c^2 we find 6,783 events. The signal to background ratio of (1.84 ± 0.10) is estimated by fitting a gaussian ($\bar{m} = 958.2 \pm 0.4$ MeV/c^2) plus a linear background. Monte Carlo simulations show that the major contribution to the background is due to the channels $\pi^0\pi^0\omega$ (10%), with $\omega\to\pi^0\gamma$ and one photon escaping the detection, $3\pi^0$ and $\pi^0\pi^0\eta$ which populate the high $\pi^0\eta'$-mass ends of the phase space as seen in the background Dalitz plot fig. 4b.

A 7C kinematic fit corresponding to the $\pi^0\pi^0\eta'$ hypothesis for events falling into the η' mass window was applied. The remaining background was subtracted following the same procedure as for the 10-photon sample. The final

Dalitz plot (3,559 events) and the side-bin Dalitz plot are shown in fig. 4a and 4b. The efficiency of the data selection and identification of the $\pi^0\pi^0\eta'$ channel in the six photon final state is $(11.7 \pm 1.9)\%$ estimated by Monte Carlo simulation, assuming a flat phase space distribution. A small decrease in efficiency is only seen in a small region at the $\pi^0\pi^0$ threshold. The branching ratio is calculated by scaling the number of events relative to the number of events attributed to $\bar{p}p \rightarrow \omega\omega$, which was selected in parallel from the 6-photon sample. The branching ratio of the latter channel was determined in [8].

For both investigations of the $\pi^0\pi^0\eta'$ final state we arrive at compatible branching ratios after correction for the η' decay according to [9] ($B_{10\gamma} = (3.2 \pm 0.5) \cdot 10^{-3}$, $B_{6\gamma} = (3.7 \pm 0.8) \cdot 10^{-3}$), and obtain the average:

$$Br(\bar{p}p \rightarrow \pi^0\pi^0\eta') = (3.34 \pm 0.42) \cdot 10^{-3}\,. \tag{1}$$

The Dalitz plots of the $\pi^0\pi^0\eta'$ final state with 10 or 6γ (fig. 2 and fig. 4) are compatible. We now describe the partial wave analysis. The kinematically allowed region for $\pi^0\pi^0$ is limited to 270–957 MeV, where the $(\pi^0\pi^0)$ S-wave can be described unambiguously as in our previous publications on $\bar{p}p \rightarrow 3\pi^0$ [2,10]. Due to the small branching ratio of $\bar{p}p \rightarrow f_2(1270)\eta$ in the $\pi^0\pi^0\eta$ data [1–3], the $f_2(1270)$ can be neglected here.

The $\pi\eta'$ mass range covers 1090 MeV to 1740 MeV where the $a_2(1320)$ and the $a_0(1450)$ may contribute. We find no visible evidence for the high energy tail of the $a_0(980)$ or the low energy tail of the $a_2'(1650)$ [1]. They both fall into the marginal zone of the Dalitz plot with low statistics and low signal to background ratio. This region has little impact on the $a_2(1320)$ and the $a_0(1450)$ since these two mesons populate the central region of the Dalitz plot. The background in this mass range is flat.

As a further amplitude, we also try the $\eta'\pi$ P-wave with exotic quantum numbers $I^G(J^{PC}) = 1^-(1^{-+})$. The GAMS collaboration has reported a resonance $\hat{\rho}(1405)$ in the reaction $\pi^- p \rightarrow \eta\pi^0 n$ [11]. In an analysis of our data on $\pi^0\pi^0\eta$, we found a contribution compatible with non-resonant behaviour [1]. Here we consider either a resonant or a non-resonant behaviour.

The amplitudes for the fit of the $\pi^0\pi^0\eta'$ Dalitz plot are formulated using the K-matrix formalism in the P-vector approach [12]. In agreement with the successful description of other three pseudoscalar final states of $\bar{p}p$ annihilation at rest and due to the limited statistics, we consider the $^1S_0$ $\bar{p}p$ initial state only and neglect P-wave annihilation. The square of the coherent sum of transition amplitudes in a certain cell of the Dalitz plot area has to reproduce the observed event density. For adjusting the production strengths, masses and widths of intermediate resonances we used MINUIT [13] minimizing the

No.	$(\pi\pi)_S$	$a_0(1450)$			$a_2(1320)$			χ^2
		m	Γ		m	Γ		
	%	[MeV]	[MeV]	%	[MeV]	[MeV]	%	
1	100	–	–	–	–	–	–	500
2	88.7 ± 3.1	1450	260	8.7 ± 2.4	–	–	–	344
3	96.9 ± 0.6	–	–	–	1320	110	2.6 ± 0.5	321
4	93.8 ± 0.4	1450	260	3.2 ± 0.6	1320	110	1.8 ± 0.4	285
5	93.1 ± 0.4	1470	265	2.7 ± 0.4	1320	110	1.4 ± 0.4	286
6	94.4 ± 1.0	1450	260	1.5 ± 1.2	1360 ± 20	160 ± 40	3.0 ± 0.5	274

Table 1
Results of the partial wave analysis of the $\pi^0\pi^0\eta'$ Dalitz plot. Branching ratios are given ignoring interferences between channels, so they do not add up to exactly 100%.

Poisson likelihood chisquare [14]:
$\chi^2 = 2\sum_i y_i - n_i + n_i \ln(n_i/y_i)$, with n_i the number of events in the i-th bin and y_i the number of events predicted by the model in the i-th bin. We quote the corresponding Neyman chisquare here. The results of the partial wave analysis applied to the 10-photon sample (246 data points) are summarized in table 1. The 6γ data sample leads to compatible results.

As a first hypothesis we assume that only the $\eta'(\pi\pi)_S$ wave contributes and neglect $\pi^0\eta'$ interactions (fit 1). This fit is obviously inadequate, since it gives uniform diagonal bands on the Dalitz plot, in clear disagreement with data (see fig. 6a). The addition of $a_0(1450)$ or $a_2(1320)$, with fixed mass and width, gives a large improvement in χ^2 (fits 2 and 3). We find a further significant improvement of $\Delta(\chi^2) = 36$ when including both resonances (fit 4). A comparison of the experimental Dalitz plot with this fit and the corresponding χ^2 distribution is given in fig. 5. The errors quoted are due to a statistical and a systematic error covering uncertainties in the mass and width of the resonance content. We omit contributions from the interference of the two $a_2(1320)$ and the two $a_0(1450)$ bands.

The influence of the $a_0(1450)$ on the quality of the fit is visible in the $\pi^0\eta'$ mass distribution fig. 6. Without $a_0(1450)$ there are deviations in the center of the $\pi^0\pi^0\eta'$ phase space.

SU(3) predicts the relative branching ratios of $a_0(1450)$ ($\rightarrow \eta'\pi^0, \eta\pi^0$) in $\eta\pi^0\pi^0$ and $\eta'\pi^0\pi^0$. It likewise predicts the magnitude of the $a_0(980)$ contribution to $\eta'\pi^0\pi^0$ using our earlier partial wave analysis of $\pi^0\pi^0\eta$. The prediction is a small $a_0(980)$ contribution ($0.7 \pm 0.1\%$) which is included in fit 5. The contributions of the $a_0(1450)$ and the $a_2(1320)$ are slightly reduced compared

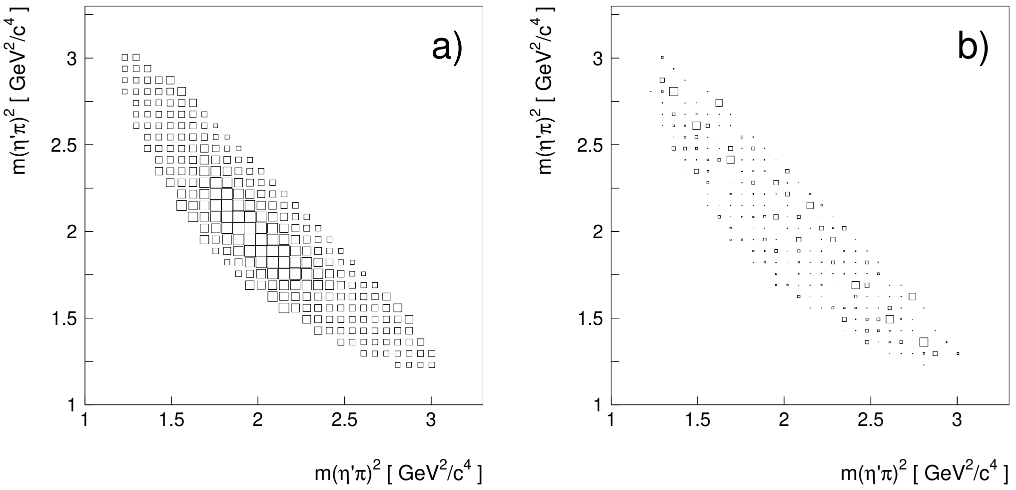

Fig. 5. *Comparison of data and fit to hypothesis 4 of the* $\pi^0\pi^0\eta'(\eta'\to\pi^0\pi^0\eta')$ *Dalitz plot: a) the theoretical Dalitz plot b) corresponding* χ^2 *distribution comparing data with fit 4. The largest boxes correspond to* χ^2 *values of 5.*

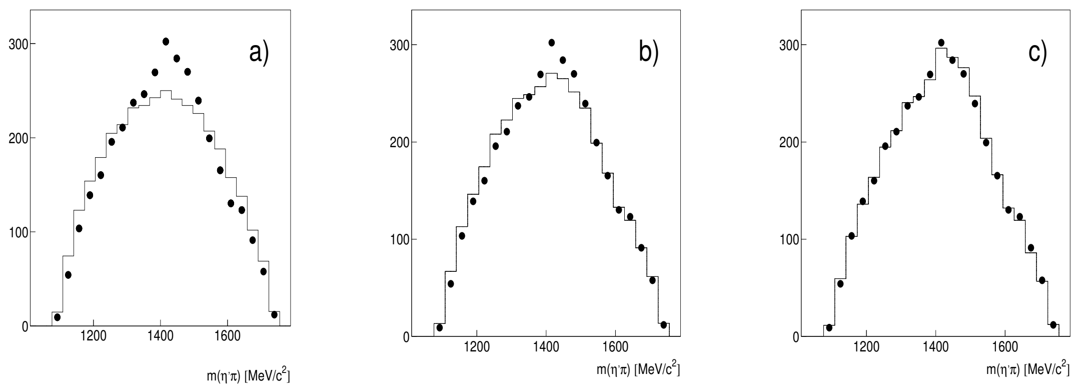

Fig. 6. *Comparison of the* $\pi^0\eta'$ *mass projection of data (dots) and fit (histogram) with a reduced binning: a)* $\pi\pi$ *S-wave tried only (fit 1), b) without* $a_0(1450)$ *(fit 3) and c) including* $a_0(1450)$ *(fit 4).*

to fit 4, but there is no improvement in χ^2.

It is not possible to get a good description of the data without $a_2(1320)$. Adding the resonating $\eta'\pi$ P-wave improves χ^2 by only 3 if fitted with GAMS parameters [11] or by 7 if fitted freely in mass and width up to non-resonant widths. However, the value of χ^2/ndf remains the same due to the additional free parameters. It removes intensity from the $a_0(1450)$ and the $\pi\pi$ S-wave, but the contribution amounts at most to 0.7%.

In fit 6 the mass and width of the $a_2(1320)$ are varied freely. However, the data are very insensitive to the $a_0(1450)$. Therefore we shall keep the mass and width of $a_0(1450)$ fixed at values from ref. [1]. The fit is not sensitive to the detailed shape of the $\pi\pi$ S-wave. Different parametrisations from other analyses do not cause changes in the fit quality and result.

We now compare the branching ratios for $a_2(1320)$ and $a_0(1450)$ with predictions of SU(3)-flavour. As a consequence of the OZI-rule, couplings of these states to the η or η' occur only via their $(\bar{d}d - \bar{u}u)$ components. This implies for the ratio of branching ratios [15]

$$\rho(\eta'\pi/\eta\pi) = \frac{F_L^2(q_{\pi^0\eta'})}{F_L^2(q_{\pi^0\eta})} \cdot \frac{q_{\pi^0\eta'}}{q_{\pi^0\eta}} \cdot \tan^2(90^\circ - \Theta_{id} + \Theta_{PS}), \tag{2}$$

with a pseudoscalar mixing angle Θ_{PS} of $(-17.3 \pm 1.8)^\circ$ from [15] and an ideal mixing angle Θ_{id} of 35.3°. The decay momenta $q_{\pi^0\eta'}$ and $q_{\pi^0\eta}$ are phase space factors. The function $F_L^2(q)$ describes the angular momentum barrier in the decay of a resonance with relative angular momentum L between the decay particles. For $L = 0$, $F_L^2(q) = 1$. The eqn.(2) predicts for $a_0(1450)$ a ratio

$$\rho(a_0(1450)) = 0.37 \pm 0.06. \tag{3}$$

The $a_2(1320)$ ratio depends strongly on $F_L^2(q)$. A simple choice is $F_L^2(q) = q^{2L}$ [16]. This is an approximation for small values of q and describes point-like particles. It results in a predicted ratio of $\rho(a_2(1320)) = 0.027$. For extended particles we use a Blatt-Weisskopf parametrisation [17],

$$F_2^2(q) = \frac{(qr)^4}{((qr)^2 - 3)^2 + 9(qr)^2} \quad . \tag{4}$$

The mean range parameter r depends on the size of the meson. For $r = 1$ fm, $\rho = 0.12$.

For the calculation of the intensity of partial waves we use fit 4 and average the results obtained for the ten-photon and six-photon samples. The $a_0(1450)$ contribution to the $\pi^0\pi^0\eta'$ channel is $(3.5 \pm 0.5)\%$. With its contribution of 4% to $\bar{p}p \rightarrow \pi^0\pi^0\eta$ [1–3] and the branching ratio of $(6.7 \pm 1.2) \cdot 10^{-3}$ [1] for $\bar{p}p \rightarrow \pi^0\pi^0\eta$, we calculate for the ratio of branching ratios (eqn.(2))

$$\rho(a_0(1450)) = \frac{Br(a_0(1450) \rightarrow \eta'\pi)}{Br(a_0(1450) \rightarrow \eta\pi)} = 0.43 \pm 0.11 \quad . \tag{5}$$

This result is in nice agreement with the SU(3) prediction (see eqn.(3)).

For the $\pi^0\pi^0$ S-wave, which contributes about 50% to $\pi^0\pi^0\eta$ and $(93.6 \pm 0.4)\%$ to $\pi^0\pi^0\eta'$, we find

$$\rho((\pi^0\pi^0)_S) = \frac{Br(\bar{\mathrm{p}}\mathrm{p}\to\eta'(\pi^0\pi^0)_S)}{Br(\bar{\mathrm{p}}\mathrm{p}\to\eta(\pi^0\pi^0)_S)} = 0.93 \pm 0.20 \ . \tag{6}$$

For two-body final states we have measured earlier the following ratios [15]:

$$Br(\bar{\mathrm{p}}\mathrm{p}\to\pi^0\eta')/Br(\bar{\mathrm{p}}\mathrm{p}\to\pi^0\eta) = 0.548 \pm 0.048 \tag{7}$$
$$Br(\bar{\mathrm{p}}\mathrm{p}\to\eta\eta')/(2\cdot Br(\bar{\mathrm{p}}\mathrm{p}\to\eta\eta)) = 0.652 \pm 0.069 \tag{8}$$
$$Br(\bar{\mathrm{p}}\mathrm{p}\to\omega\eta')/Br(\bar{\mathrm{p}}\mathrm{p}\to\omega\eta) = 0.515 \pm 0.031 \tag{9}$$

Thus the behaviour of the $(\pi^0\pi^0)$ S-wave is similar to two-body processes involving an η or η'.

We found 30% $a_2(1320)$ intensity in the $\pi^0\pi^0\eta$ final state [1–3]. From its contribution of (1.9 ± 0.3)% to $\pi^0\pi^0\eta'$ one obtains

$$\rho(a_2(1320)) = \frac{Br(a_2(1320)\to\eta'\pi)}{Br(a_2(1320)\to\eta\pi)} = 0.032 \pm 0.009 \ . \tag{10}$$

This is in agreement with two measurements of the VES collaboration [18,19] quoting a ratio of $\rho = 0.047 \pm 0.010 \pm 0.004$ and $\rho = 0.034 \pm 0.008 \pm 0.005$, respectively. For the mean of the three values we find

$$\rho(a_2(1320)) = 0.037 \pm 0.006 \ . \tag{11}$$

According to eqn.(4) this value implies a weak centrifugal barrier for $\bar{p}p \to a_2(1320)\pi$, namely an upper limit of $r = 0.40$ fm. For other tensor mesons, a value of (0.20 ± 0.04) fm for r was determined in ref. [20].

$BR(\bar{p}p\to PS\,X; X\to (PS)(PS))$	$\cdot 10^{-3}$
$\bar{p}p\to a_0(1450)\pi^0; a_0(1450)\to \pi^0\eta'$	0.117 ± 0.022
$\bar{p}p\to a_2(1320)\pi^0; a_2(1320)\to \pi^0\eta'$	0.064 ± 0.013
$\bar{p}p\to (\pi\pi)_S\eta'; (\pi\pi)_S\to \pi^0\pi^0$	3.1 ± 0.4

Table 2
Product branching ratios

We conclude, that the $\pi^0\pi^0\eta'$ and the $\pi^0\pi^0\eta$ final states of $\bar{p}p$ annihilation at rest are consistent with the production of both $I = 1$ resonances $a_0(1450)$ and $a_2(1320)$ and with rates compatible with SU(3)-flavor expectations. The branching fractions are given in table 2. A small amount of exotic P-wave can be introduced in addition to the $\pi\pi$ S-wave, $a_0(1450)$ and $a_2(1320)$. The resonance parameters of $a_2(1320)$ are better defined in the Dalitz plot analysis than these of $a_0(1450)$.

We wish to thank the technical staff of the LEAR machine group and of all the participating institutions for their invaluable contributions to the success of the experiment. We acknowledge financial support from the German Bundesministerium für Bildung, Wissenschaft, Forschung und Technologie, the Schweizerischer Nationalfonds, the British Particle Physics and Astronomy Research Council, the KFA Jülich, the U.S. Department of Energy and the National Science Research Fund Committee of Hungary (contract No. DE-FG03-87ER40323, DE-AC03-76SF00098, DE-FG02-87ER40315 and OTKA F014357). N. Djaoshvili, F.-H. Heinsius and K.M. Crowe acknowledge support from the A. von Humboldt Foundation.

References

[1] C. Amsler et al., Phys. Lett. **B333** (1994) 277

[2] C. Amsler et al., Phys. Lett. **B355** (1995) 425

[3] A. Abele et al., Nucl. Phys.**A609** (1996) 562

[4] A. Abele et al., Phys. Lett. **B380** (1996) 453

[5] C. Amsler et al., Phys. Lett. **B340** (1994) 259

[6] E. Aker et al., Nucl. Instr. Meth. **A321** (1992) 69

[7] C. Amsler et al., Phys. Lett. **B358** (1995) 389

[8] C. Amsler et al., Z. Phys. **C 42** (1993) 175

[9] Review of Particle Physics, Phys. Rev. **D54** (1996) 1

[10] C. Amsler et al., Phys. Lett. **B342** (1995) 433

[11] M. Boutemeur, M. Poulet, Hadron '89, ed. F. Binon, J.M. Frère, J.P. Peigneux - (Ed. Frontières 1989) p. 119

[12] S.U. Chung et al., Ann. Phys. **4** (1995) 404

[13] F.James and M. Roos, CERN Library long writeup D506, 1987

[14] S. Baker and R.D. Cousins, Nucl. Instr. Meth. **221** (1984) 437

[15] C. Amsler et al., Phys. Lett. **B294** (1992) 451

[16] C.B. Dover, P.M. Fishbane, Nucl. Phys. **B244** (1984) 349

[17] F. V. Hippel, C. Quigg, Phys. Rev. **5** (1972) 624

[18] G.M. Beladidze et al., Z. Phys. **C54** (1992) 235

[19] G.M. Beladidze et al., Phys. Lett. **B313** (1993) 276

[20] K. Peters, E. Klempt, Phys. Lett. **B352** (1995) 467